

Pancreas dorsal lobe agenesis and abnormal islets of Langerhans in *Hlxb9*-deficient mice

Kathleen A. Harrison¹, Joshua Thaler², Samuel L. Pfaff², Hua Gu³ & John H. Kehrl¹

In most mammals the pancreas develops from the foregut endoderm as ventral and dorsal buds. These buds fuse and develop into a complex organ composed of endocrine, exocrine and ductal components^{1,2}. This developmental process depends upon an integrated network of transcription factors. Gene targeting experiments have revealed critical roles for *Pdx1*, *Isl1*, *Pax4*, *Pax6* and *Nkx2-2* (refs 3–10). The homeobox gene *HLXB9* (encoding HB9) is prominently expressed in adult human pancreas¹¹, although its role in pancreas development and function is unknown. To facilitate its study, we isolated the mouse *HLXB9* orthologue, *Hlxb9*. During mouse development, the dorsal and ventral pancreatic buds and mature β -cells in the islets of Langerhans express *Hlxb9*. In mice homologous for a null mutation of *Hlxb9*, the dorsal lobe of the pancreas fails to develop. The remnant *Hlxb9*^{-/-} pancreas has small islets of Langerhans with reduced numbers of insulin-producing β -cells. *Hlxb9*^{-/-} β -cells express low levels of the glucose transporter *Glut2* and homeodomain factor *Nkx 6-1*. Thus, *Hlxb9* is key to normal pancreas development and function.

We isolated mouse *Hlxb9* cDNA and genomic clones using nucleotide sequence information from the human *HLXB9* cDNA. The predicted mouse protein shares with human HB9 (ref. 11) a glycine- and alanine-rich region to the amino-terminal side of the homeodomain and a strongly acidic region carboxy terminal to the homeodomain. Northern-blot analysis revealed a 2.4-kb transcript present in adult mouse pancreas and testis (data not shown). Using a specific antiserum, we detected Hb9 in the nuclei of cells in the islets of Langerhans, but not in the exocrine portion of adult mouse pancreas (Fig. 1a). Most islet endocrine cells expressed Hb9, although a few showed no reactivity. Analysis of adult pancreas simultaneously reacted with an insulin-specific antibody and the Hb9 antiserum indicated that all islet cells that expressed insulin also expressed Hb9 (Fig. 1b). A similar analysis with glucagon, somatostatin and pancreatic polypeptide-specific antisera revealed that nuclei of islet cells reactive with these antibodies did not co-express Hb9 (Fig. 1c). These results indicate that Hb9 expression is restricted to β -cells in the adult mouse pancreas.

To determine when during embryogenesis Hb9 is expressed in pancreatic tissue, we performed immunohistochemistry with slides prepared from transverse sections of staged mouse embryos. In embryonic day (E) 9.5 embryos, Hb9 was detected in the nuclei of cells in the notochord, spinal cord and the epithelium of the fore- and midgut, where it was present in a dorsal to ventral gradient (Fig. 2a, and data not shown). The region of the developing dorsal pancreatic bud expressed high levels of Hb9 and showed the expected distri-

bution of *Isl1*-positive cells in the mesenchyme⁶ (Fig. 4). By E10.5, Hb9 was detected in both the dorsal and ventral pancreatic buds. The expected distribution of *Isl1* and *Pdx1* in the dorsal and ventral buds is also shown, as well as a section demonstrating expression of Hb9 in both buds (Fig. 2b–h). By E12.5, the levels of Hb9 and *Isl1* declined, whereas the developing dorsal and ventral buds continued to express *Pdx1* (Fig. 2i–k). A day later, cells expressing high levels of Hb9 were again present in the ventral and dorsal portion of the pancreas (Fig. 2l), and by E17.5 they were restricted to the developing islets of Langerhans (Fig. 2m,n). In E13.5 exocrine pancreas, we detected low levels of Hb9 in some nuclei, but they became progressively less apparent in older embryos. Besides the developing pancreas, the epithelium of the developing oesophagus, stomach and small intestine also expressed Hb9 (data not shown).

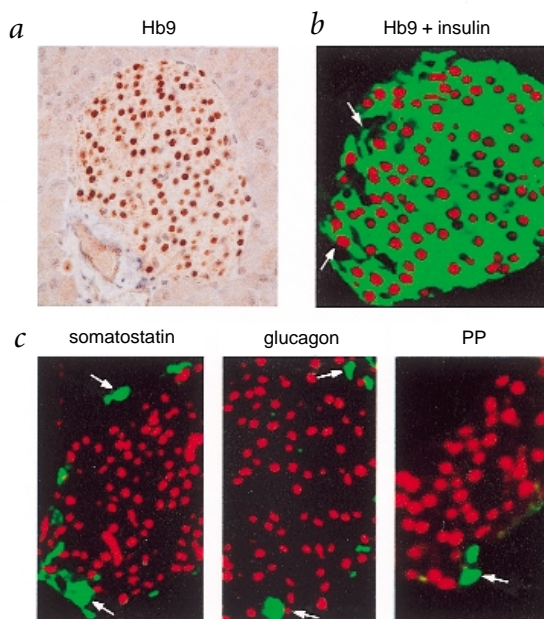


Fig. 1 Hb9 in the islets of Langerhans of adult mice. **a**, Hb9 in adult pancreas. Immunocytochemistry was performed on paraffin sections prepared from mouse pancreas using Hb9-specific antiserum (photographed at $\times 400$). The slide was counterstained with haematoxylin. **b**, Hb9 and insulin co-localize in pancreatic islet cells. Overlaid digital images of adult mouse pancreas stained with a mouse monoclonal antibody against insulin (green) and rabbit anti-Hb9 antiserum (red). Hb9-negative and insulin-negative islet cells are indicated with arrows. **c**, Hb9 is restricted to β cells. Overlaid digital images adult of mouse pancreas stained to detect somatostatin (left), glucagon (middle) and pancreatic polypeptide (right), all in green, and Hb9 in red. Hb9-negative hormone-positive cells are indicated with arrows.

¹Laboratory of Immunoregulation and ³Laboratory of Immunology, National Institute of Allergy and Infectious Diseases, National Institutes of Health, Bethesda, Maryland 20892, USA. ²Gene Expression Laboratory, the Salk Institute for Biological Studies, La Jolla, California 92037, USA. Correspondence should be addressed to J.H.K. (e-mail: jkehrl@niaid.nih.gov).

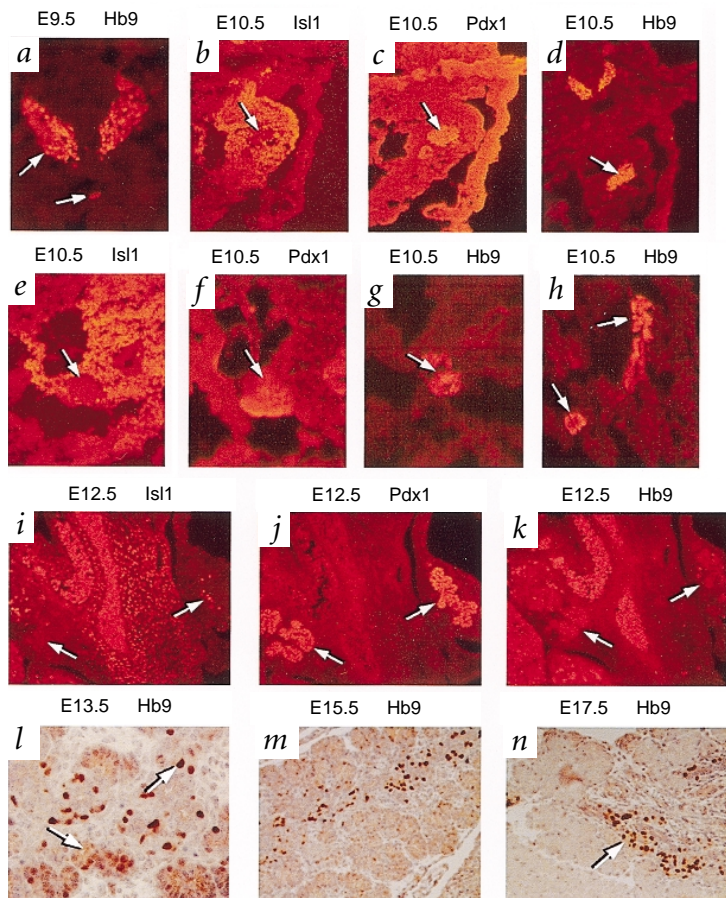


Fig. 2 Hb9 is expressed in the developing pancreas. **a**, Hb9 expression in the spinal cord and notochord of an E9.5 embryo (photographed at $\times 400$). **b-d**, Hb9 expression in the dorsal pancreatic bud. Adjacent transverse sections through an E10.5 embryo reacted with antisera against Isl1 (**b**), Pdx1 (**c**) or Hb9 (**d**; photographed at $\times 400$). Arrows point to the dorsal bud. **e-g**, Hb9 expression in the ventral pancreatic bud. Adjacent transverse sections through an E10.5 embryo reacted with antisera against Isl1 (**e**), Pdx1 (**f**) or Hb9 (**g**; photographed at $\times 400$). Arrows point to the ventral pancreatic bud. **h**, Hb9 expression in dorsal and ventral buds. Transverse section through an E10.5 embryo reacted with the Hb9 antiserum (dorsal and ventral buds indicated by top and bottom arrows, respectively). **i-k**, Hb9 levels decline in E12.5 embryos. Adjacent transverse sections from an E12.5 embryo reacted with antisera against Isl1, Pdx1 and Hb9 (photographed at $\times 200$). Autofluorescent red cells account for the background. Arrows show the developing pancreatic lobes. **l-n**, Hb9 localizes to the islets of Langerhans. Transverse sections through E13.5, E15.5 and E17.5 reacted with antisera against Hb9 (photographed at $\times 400$, $\times 200$ and $\times 200$, respectively). In the E13.5 embryo, the top arrow points to a developing islet cell, the bottom one to the exocrine pancreas.

shown (Fig. 3a). Mice heterozygous for the *Hlxb9* mutation had no apparent abnormalities, but they had no viable *Hlxb9*^{-/-} offspring. Analysis of embryos from interrupted term pregnancies revealed the expected mendelian frequencies of mutant genotypes, indicating that homozygous mutants died at the time of birth. An analysis of the cause of death and the role of *Hlxb9* in motor neuron development is the subject of another report¹⁴. Term *Hlxb9*^{-/-} embryos had no obvious morphological abnormality, except for a slightly smaller and more curled appearance than their littermates (Fig. 3b). Despite their curled body and the established role of *HLXB9* in sacral agenesis¹⁵, skeletal development in *Hlxb9*^{+/-} and *Hlxb9*^{-/-} mice appeared normal, as assessed by differential staining of cartilage and bone using Alcian blue and Alizarin red and by X-ray (data not shown). Early B and T lymphocyte development in *Hlxb9*^{-/-} mice appeared intact, although we noted a modest reduction in fetal liver myeloid progenitors (C. Moratz, unpublished data).

To examine the role of *Hlxb9* in pancreas development and function, we generated mice that lack exon 3 of *Hlxb9*, which encodes the C-terminal portion of the homeodomain and the remainder of the protein. We deleted exon 3 by inserting flanking *loxP* sites by homologous recombination in ES cells followed by expression of the Cre recombinase^{12,13}. A schematic of the *Hlxb9* locus and the targeting construct is

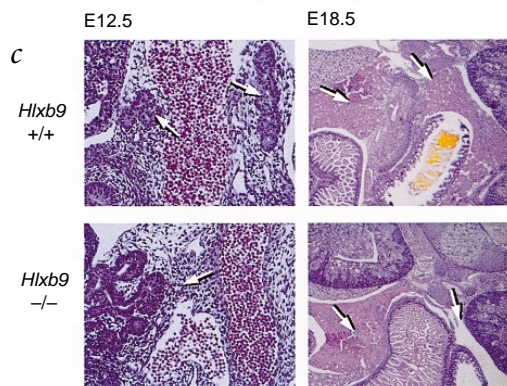
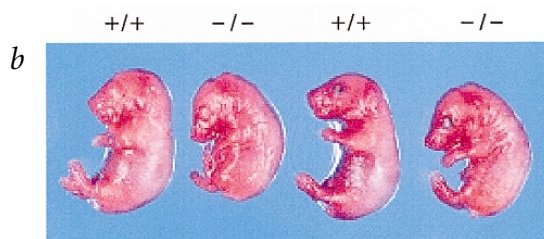
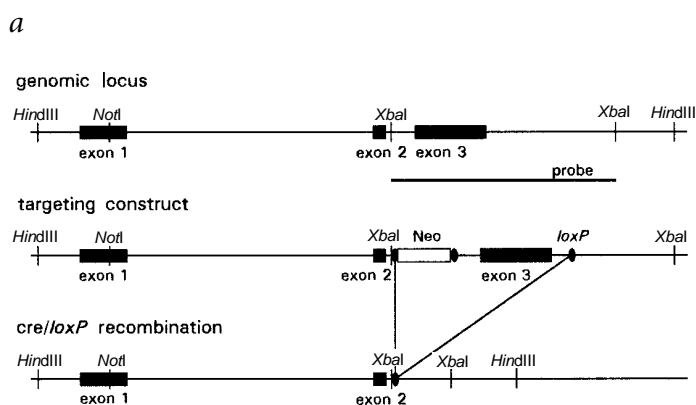
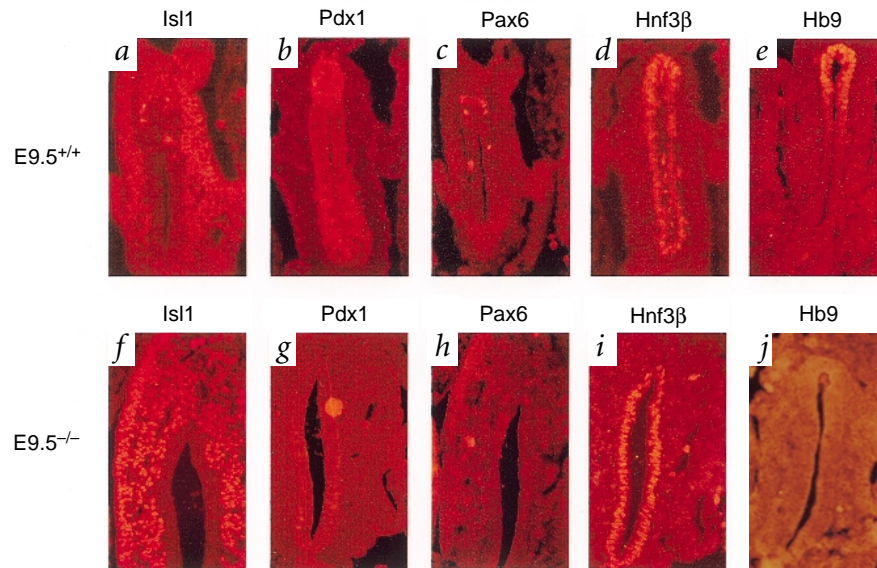


Fig. 3 The dorsal lobe of the pancreas fails to develop in *Hlxb9*^{-/-} mice. **a**, Targeted deletion of exon 3 of *Hlxb9*. The structure of the wild-type and targeted *Hlxb9* loci is shown. **b**, Comparison of wild-type and *Hlxb9*^{-/-} E18.5 embryos. Genotypes are indicated above the photograph. **c**, H&E stain of transverse sections of wild-type and *Hlxb9*^{-/-} E12.5 and E18.5 embryos. The dorsal and ventral lobes of the pancreas in wild-type mice and the ventral lobe of the pancreas in the *Hlxb9*^{-/-} mice are indicated (E18.5 photographed at $\times 400$, E12.5 at $\times 1,000$). The expected location of the dorsal lobe of the pancreas (right arrow) is indicated. Serial sections failed to identify any remnant of the dorsal lobe in the *Hlxb9*^{-/-} mutants.

Fig. 4 Expression of Pdx1, Isl1, Pax6 and Hnf3 β in *Hlxb9*^{-/-} mice. *a–i*, Expression in wild-type and *Hlxb9*^{-/-} mice at the expected level of the dorsal bud. Adjacent transverse sections of E9.5 wild-type and *Hlxb9*^{-/-} mice reacted with antisera against Isl1 (*a,f*), Pdx1 (*b,g*), Pax6 (*c,h*), Hnf3 β (*d,i*) or Hb9 (*e,j*). All sections were photographed at $\times 200$.



To analyse pancreas development in the mutants, we examined serial transverse sections through the foregut and midgut regions prepared from E12.5, E15.5, E17.5 or E18.5 mice. In *Hlxb9*^{-/-} mice the dorsal lobe of the pancreas was never seen, whereas the ventral lobe appeared as expected (Fig. 3c). To determine whether the dorsal bud of the pancreas is present but fails to develop, we exam-

ined serial transverse sections from E9.5 embryos. As expected, we saw cells expressing Isl1, Pdx1 and Hb9 in the dorsal pancreatic epithelium of wild-type mice (Fig. 4*a,b,e*), but such cells were not seen at the expected level in endoderm of *Hlxb9*^{-/-} mice (Fig. 4*f,g*). *Hlxb9*^{-/-} mesenchymal cells that should envelop the developing dorsal pancreatic epithelium did express Isl1 (Fig. 4*f*). We also

examined *Hlxb9*^{-/-} mice for the expression of two other transcription factors implicated in pancreas development, Pax6 and Hnf3 β (refs 7–9,16). We detected Hnf3 β expression in the dorsal pancreatic epithelium of both wild-type and *Hlxb9*^{-/-} mice, but although we observed scattered Pax6-positive cells in wild-type mice, we did not see such cells in *Hlxb9*^{-/-} mice (Fig. 4*c,d,h,i*). As expected, we did not detect Hb9 expression in sections prepared from the homozygous mutants (Fig. 4*j*). The ventral pancreatic bud appeared in *Hlxb9*^{-/-} mice and expressed Pdx1, as expected (data not shown).

To determine whether *Hlxb9* has a role in the differentiation of cells in the islets of Langerhans, we examined the remaining portion of the pancreas in *Hlxb9*^{-/-} mice for insulin, pancreatic polypeptide, glucagon and somatostatin expression. We found all four types of hormone-producing cells (α , β , δ and γ) in *Hlxb9*^{-/-} islets of Langerhans (Fig. 5*a*). A comparison of the number of hormone-producing cells

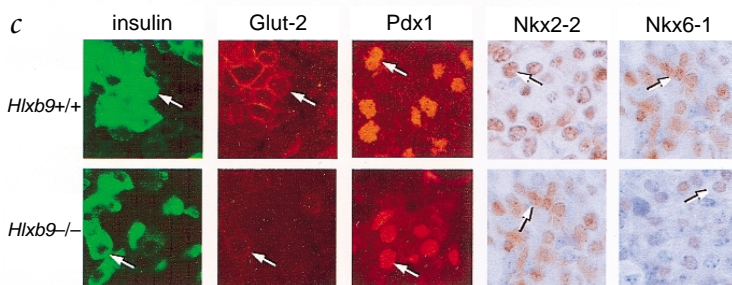
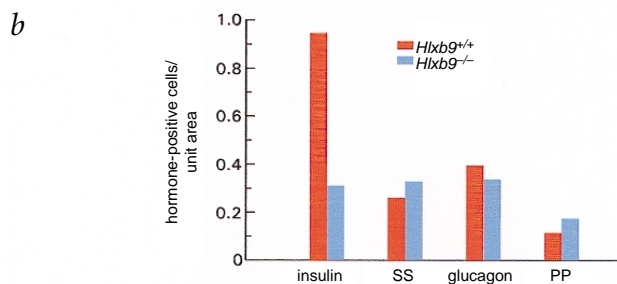
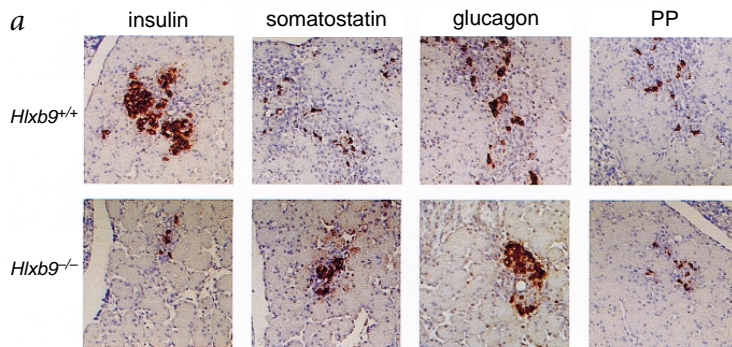


Fig. 5 Abnormal islets of Langerhans in *Hlxb9*^{-/-} mice. *a*, Insulin, somatostatin, glucagon and pancreatic polypeptide (PP) expression in E18.5 wild-type and *Hlxb9*^{-/-} mice. Transverse sections from wild-type and *Hlxb9*^{-/-} littermates were reacted with guinea pig anti-insulin, rabbit anti-somatostatin, rabbit anti-glucagon or rabbit anti-PP antisera. Positive cells are dark brown, photographed at $\times 200$. *b*, Density of hormone-producing cells per unit area of ventral pancreas. Density from E18.5 pancreas from wild-type and *Hlxb9*^{-/-} mice was quantified from digital images acquired from multiple slides stained for the indicated hormones. *c*, Analysis of *Hlxb9*^{-/-} β -cells. Transverse sections from E18.5 wild-type and *Hlxb9*^{-/-} littermates were reacted with antisera against insulin, Glut2, Pdx1, Nkx2-2 and Nkx6-1. Insulin (green) and Glut2 (red) expression were analysed by double immunofluorescence (insulin-positive cells and the corresponding cells expressing Glut2 in the adjacent image are indicated with arrows). Pdx1 was detected by immunofluorescence (red), Nkx2-2 and Nkx6-1 by ABC kit (positive nuclei are brown and representative nuclei are indicated with arrows). Photographed at $\times 1,000$.

per unit area of ventral exocrine pancreas in E18.5 wild-type and *Hlxb9*^{-/-} mice revealed a 65% reduction in insulin-positive (β) cells (Fig. 5b). We did not see a difference in the densities of the other hormone-producing cells. The reduction in the size of the islets from *Hlxb9*^{-/-} mice likely occurs as a consequence of decreased numbers of β -cells. The islets of wild-type mice averaged 5.5 \pm 1.2% of their ventral lobes, whereas the islets in *Hlxb9*^{-/-} mice averaged 2.3 \pm 1.4% of their ventral lobes as assessed by digitally analysing sections prepared from 9 wild-type and 9 *Hlxb9*^{-/-} animals. In addition, the normal peripheral location of the non- β hormone cells in the islets of Langerhans was disrupted in *Hlxb9*^{-/-} mice. We also noted an increased intensity of somatostatin staining in the islets of *Hlxb9*^{-/-} mutants (Fig. 5a).

Further analysis of *Hlxb9*^{-/-} β -cells (Fig. 5c) revealed that they expressed much lower levels of Glut2, the low-affinity glucose transporter normally present in the plasma membrane of β -cells¹⁷, and modestly lower levels of Nkx6-1, a homeodomain factor expressed exclusively in β -cells in E18 mice¹⁸. Glut2 expression is known to be absent in *Nkx2-2*^{-/-} β -cells¹⁰ and to be reduced in *Pdx1*-deficient β -cells¹⁹, but we detected both of these transcription factors as well as Isl1 in E18 *Hlxb9*^{-/-} β -cells (Fig. 5c, and data not shown). The reduction of Glut2 and Nkx6-1 in the insulin-positive islet cells of *Hlxb9*^{-/-} embryos suggests that they are functionally impaired and raises the possibility that *Glut2* and *Nkx6-1* may be direct or indirect target genes of Hb9.

The *Hlxb9* targeting experiment shows that the dorsal lobe of the pancreas does not develop in the absence of *Hlxb9*. The lack of *Pdx1* and *Isl1* expression in the dorsal pancreatic epithelium suggests that *Hlxb9* may be important for early cell fate decisions. The dorsal pancreatic mesenchyme in *Hlxb9*^{-/-} mice appears intact and expresses normal levels of *Isl1*, suggesting that the failure of dorsal lobe development is not likely to be secondary to deficient signals from the mesenchyme. Because of the importance of notochord-derived signals in development of the dorsal lobe of the pancreas^{20–22}, the absence of *Hlxb9* in the notochord could alter notochord function, resulting in defective signals to the dorsal pancreatic epithelium. However, the fact that *Hlxb9*^{-/-} notochord appears morphologically normal and patterns the neural tube and somites correctly, and that Sonic hedgehog expression is repressed in *Hlxb9*^{-/-} pancreatic endoderm as expected (K.A.H., unpublished data), makes this seem less likely. Nevertheless, the activation of a signalling molecule by Hb9 remains a possible explanation for the phenotype we observe.

A complicated interplay between different transcription factors and their target genes is responsible for lineage specification and differentiation of the cell types that comprise the exocrine and endocrine portions of the pancreas^{23,24}. Final cell fate may be specified by a transcription factor code as proposed for the differentiation of motor neurons²⁵. Besides their role in pancreas development, both *Isl1* and *Hlxb9* are required for the generation of motor neurons^{14,26}. Thus, the transcriptional control elements that regulate motor neuron and pancreatic differentiation appear to be targets of an overlapping set of transcription factors.

Methods

Characterization of mouse *Hlxb9* and cDNA cloning. We subjected mouse genomic DNA to PCR using primers derived from exon 2 of human *HLXB9* (5' primer, 5'-CACGCGCAGTCGAACCTCCTG-3'; 3' primer, 5'-CTG GGTCTCGGTGAGCATGAG-3'). This generated the expected 160-bp product, which we subcloned into pCRII. Its nucleotide sequence closely matched that of human *HLXB9*. Using the same set of primers, we isolated two clones from a mouse P1 genomic library (Genome Systems), from which we subcloned a 9-kb *HindIII* fragment that spanned mouse *Hlxb9* into

pBluescript (Stratagene) and determined its sequence. A comparison of the mouse and human sequences revealed that the original PCR primers had two mismatches, one at the third base from the 3' end of the 5' primer (C \rightarrow T), the other at the fourth base from the 5' end of the 3'-primer (G \rightarrow A). We obtained a full-length *Hlxb9* cDNA by RT-PCR using a cDNA prepared from E15 mouse embryo mRNA (Clontech) and appropriate PCR primers.

***Hlxb9* gene targeting.** A *Hlxb9* 5-kb *HindIII/XbaI* fragment and a 4-kb *XbaI* fragment containing exon 3 and an inserted *loxP* site flanked the neomycin-resistance gene in the pL2-neo *Hlxb9* targeting vector. To generate the targeted embryonic stem (ES) cell clones, we electroporated 30 μ g of linearized targeting vector into E14.1 ES cells and identified two correctly targeted clones. We transiently transfected them with a Cre recombinase expression vector to remove the neomycin-resistance gene and exon 3 of *Hlxb9*. After verifying the deletion, we injected ES cells into C57BL/6J blastocysts. We bred and maintained the mice under pathogen-free conditions in accordance with institutional guidelines.

Immunohistochemistry. Appropriately timed mouse embryos from interrupted pregnancies (day of plug E0.5) were fixed in 4% paraformaldehyde, paraffin embedded and 5- μ m sections mounted on slides (American HistoLabs, Inc.). We de-waxed, rehydrated and, in some instances, subjected the slides to antigen retrieval by microwaving them for 20 min in a pressure cooker with Dako target retrieval solution plus 0.1% Tween 20. After cooling in 50 mM TBS/5% BSA, we blocked the slides for 1 h with Dako blocking solution, stained them overnight with the primary antibody and detected the signal the following day by incubating for 2 h with the secondary antibody. Besides the paraffin sections, we also prepared frozen sections from some of the timed embryos²⁵. We raised Hb9 antisera by immunizing rabbits with an HB9 peptide corresponding to residues 310–405 of the predicted mouse protein (1:8,000 dilution). We used the following primary antibodies: guinea pig anti-insulin (Dako, 1:150); rabbit anti-glucagon (Dako, 1:75); rabbit anti-somatostatin (Dako, 1:300); rabbit anti-pancreatic polypeptide (Dako, 1:700); rabbit anti-PDX1 (a gift from C. Wright, 1:1,000); mouse mAb anti-Pax6 (Developmental Studies Hybridoma Bank, 1:25); rabbit anti-Isl1 (K5, 1:2,000); mouse mAb anti-HNF3 β (Developmental Studies Hybridoma Bank, 1:25); mouse mAb anti-insulin (Sigma, 1:1,000); mouse mAb anti-somatostatin (Biomed, undiluted); rabbit anti-Glut2 (Alpha Diagnostic International, 2 μ g/ml); rabbit anti-Nkx6.1 (a gift from M. German, 1:5,000); mouse mAb anti-Nkx 2.2 (Developmental Studies Hybridoma Bank, 1:25); mouse mAb anti-glucagon (Sigma, 1:2,000). Secondary antibodies (all from Jackson Laboratories) included anti-rabbit Ig conjugated to cyanine3 (1:800); anti-mouse Ig conjugated to cyanine3 (1:800); anti-mouse Ig conjugated to fluorescein (1:50). We also detected the primary antibody using a Vectastain Elite ABC kit (Vector Laboratories). We performed double immunofluorescence with the indicated primary antibodies and FITC-conjugated and cyanine3-conjugated secondary antibodies. To examine islet cell hormone production, we reacted transverse sections from wild-type and *Hlxb9*^{-/-} littermates with hormone specific antisera and then detected reactivity with the Vectastain Elite ABC kit. We counted the numbers of insulin-, somatostatin-, glucagon- and PP-positive cells in 2 transverse sections from each of 5 wild-type and 5 *Hlxb9*^{-/-} E18.5 embryos using only the ventral portion of the pancreas of the wild-type embryos. We determined the area of pancreas in each slide using a digital camera.

GenBank accession number. *Hlxb9* cDNA, AF153046.

Acknowledgements

We thank M. Rust for excellent editorial assistance, A. Walsh for performing the blastocyte injection and A.S. Fauci for continued support.

Received 12 March; accepted 4 August 1999.

1. Githens, S. Differentiation and development of the pancreas in animals. in *The Pancreas: Biology, Pathobiology, and Disease* (ed. Go, V.L.W.) 21–55 (Raven Press, New York, 1993).
2. Slack, J.M. Developmental biology of the pancreas. *Development* **121**, 1569–80 (1995).
3. Jonsson, J., Carlsson, L., Edlund, T. & Edlund, H. Insulin-promoter-factor 1 is required for pancreas development in mice. *Nature* **371**, 606–609 (1994).
4. Ahlgren, U., Jonsson, J. & Edlund, H. The morphogenesis of the pancreatic mesenchyme is uncoupled from that of the pancreatic epithelium in IPF1/PDX1-deficient mice. *Development* **122**, 1409–1416 (1996).
5. Offield, M.F. et al. PDX-1 is required for pancreatic outgrowth and differentiation of the rostral duodenum. *Development* **122**, 983–995 (1996).
6. Ahlgren, U., Pfaff, S.L., Jessell, T.M., Edlund, T. & Edlund, H. Independent requirement for ISL1 in formation of pancreatic mesenchyme and islet cells. *Nature* **385**, 257–260 (1997).
7. Sosa-Pineda, B., Chowdhury, K., Torres, M., Oliver, G. & Gruss, P. The Pax4 gene is essential for differentiation of insulin-producing β cells in the mammalian pancreas. *Nature* **386**, 399–402 (1997).
8. St-Onge, L., Sosa-Pineda, B., Chowdhury, K., Mansouri, A. & Gruss, P. Pax6 is required for differentiation of glucagon-producing α -cells in mouse pancreas. *Nature* **387**, 406–409 (1997).
9. Sander, M. et al. Genetic analysis reveals that PAX6 is required for normal transcription of pancreatic hormone genes and islet development. *Genes Dev.* **11**, 1662–1673 (1997).
10. Sussel, L. et al. Mice lacking the homeodomain transcription factor Nkx2.2 have diabetes due to arrested differentiation of pancreatic β cells. *Development* **125**, 2213–2221 (1998).
11. Harrison, K.A., Druey, K.M., Deguchi, Y., Tuscano, J.M. & Kehrl, J.H. A novel human homeobox gene distantly related to proboscipedia is expressed in lymphoid and pancreatic tissues. *J. Biol. Chem.* **269**, 19968–19975 (1994).
12. Baubonis, W. & Sauer, B. Genomic targeting with purified Cre recombinase. *Nucleic Acids Res.* **21**, 2025–2029 (1993).
13. Gu, H., Zou, Y.R. & Rajewsky, K. Independent control of immunoglobulin switch recombination at individual switch regions evidenced through Cre-loxP-mediated gene targeting. *Cell* **73**, 1155–1164 (1993).
14. Thaler, J. et al. Active suppression of interneuron programs within developing motor neurons revealed by the analysis of homeodomain factor HB9. *Neuron* (in press).
15. Ross, A.J. et al. A homeobox gene, HLXB9, is the major locus for dominantly inherited sacral agenesis. *Nature Genet.* **20**, 358–361 (1998).
16. Wu, K.L. et al. Hepatocyte nuclear factor 3 β is involved in pancreatic β -cell-specific transcription of the pdx-1 gene. *Mol. Cell. Biol.* **17**, 6002–6013 (1997).
17. Thorens, B., Sarkar, H.K., Kaback, H.R. & Lodish, H.F. Cloning and functional expression in bacteria of a novel glucose transporter present in liver, intestine, kidney, and β -pancreatic islet cells. *Cell* **55**, 281–290 (1988).
18. Jensen, J., Serup, P., Karlsen, C., Nielsen, T.F. & Madsen, O.D. mRNA profiling of rat islet tumors reveals Nkx 6.1 as a β -cell-specific homeodomain transcription factor. *J. Biol. Chem.* **271**, 18749–18758 (1996).
19. Ahlgren, U., Jonsson, J., Jonsson, L., Simu, K. & Edlund, H. β -cell-specific inactivation of the mouse *Ipf1/Pdx1* gene results in loss of the β -cell phenotype and maturity onset diabetes. *Genes Dev.* **12**, 1763–1768 (1998).
20. Kim, S.K., Hebrok, M. & Melton, D.A. Notochord to endoderm signaling is required for pancreas development. *Development* **124**, 4243–4252 (1997).
21. Hebrok, M., Kim, S.K. & Melton, D.A. Notochord repression of endodermal Sonic hedgehog permits pancreas development. *Genes Dev.* **12**, 1705–1713 (1998).
22. Apelqvist, A., Ahlgren, U. & Edlund, H. Sonic hedgehog directs specialized mesoderm differentiation in the intestine and pancreas. *Curr. Biol.* **7**, 801–804 (1997).
23. Rudnick, A., Ling, T.Y., Odagiri, H., Rutter, W.J. & German, M.S. Pancreatic β cells express a diverse set of homeobox genes. *Proc. Natl Acad. Sci. USA* **91**, 12203–12207 (1994).
24. Sander, M. & German, M.S. The β -cell transcription factors and development of the pancreas. *J. Mol. Med.* **75**, 327–340 (1997).
25. Thor, S., Andersson, S.G., Tomlinson, A. & Thomas, J.B. A LIM-homeodomain combinatorial code for motor-neuron pathway selection. *Nature* **397**, 76–80 (1999).
26. Pfaff, S.L., Mendelsohn, M., Stewart, C.L., Edlund, T. & Jessell, T.M. Requirement for LIM homeobox gene *Isl1* in motor neuron generation reveals a motor neuron-dependent step in interneuron differentiation. *Cell* **84**, 309–320 (1996).